doi:10.1093/brain/awv067 BRAIN 2015: 138; 1208–1222 | 1208

BRAIN
A JOURNAL OF NEUROLOGY

Astrocyte uncoupling as a cause of human temporal lobe epilepsy

Peter Bedner,[1] Alexander Dupper,[1] Kerstin Hüttmann,[1] Julia Müller,[1] Michel K. Herde,[1] Pavel Dublin,[1,#] Tushar Deshpande,[1] Johannes Schramm,[2] Ute Häussler,[3] Carola A. Haas,[3] Christian Henneberger,[1,4] Martin Theis[1] and Christian Steinhäuser[1]

Glial cells are now recognized as active communication partners in the central nervous system, and this new perspective has rekindled the question of their role in pathology. In the present study we analysed functional properties of astrocytes in hippocampal specimens from patients with mesial temporal lobe epilepsy without ($n = 44$) and with sclerosis ($n = 75$) combining patch clamp recording, K^+ concentration analysis, electroencephalography/video-monitoring, and fate mapping analysis. We found that the hippocampus of patients with mesial temporal lobe epilepsy with sclerosis is completely devoid of *bona fide* astrocytes and gap junction coupling, whereas coupled astrocytes were abundantly present in non-sclerotic specimens. To decide whether these glial changes represent cause or effect of mesial temporal lobe epilepsy with sclerosis, we developed a mouse model that reproduced key features of human mesial temporal lobe epilepsy with sclerosis. In this model, uncoupling impaired K^+ buffering and temporally preceded apoptotic neuronal death and the generation of spontaneous seizures. Uncoupling was induced through intraperitoneal injection of lipopolysaccharide, prevented in Toll-like receptor4 knockout mice and reproduced *in situ* through acute cytokine or lipopolysaccharide incubation. Fate mapping confirmed that in the course of mesial temporal lobe epilepsy with sclerosis, astrocytes acquire an atypical functional phenotype and lose coupling. These data suggest that astrocyte dysfunction might be a prime cause of mesial temporal lobe epilepsy with sclerosis and identify novel targets for anti-epileptogenic therapeutic intervention.

1 Institute of Cellular Neurosciences and Medical Faculty, University of Bonn, Sigmund-Freud-Str. 25, 53105 Bonn, Germany
2 Department of Neurosurgery, Medical Faculty, University of Bonn, Sigmund-Freud-Str. 25, 53105 Bonn, Germany
3 Experimental Epilepsy Research, Department of Neurosurgery, University Hospital Freiburg, 79106 Freiburg, Germany
4 UCL Institute of Neurology, UCL, London WC1N 3BG, UK
[#]Current address: Institute of Neurobiology, University of Düsseldorf, Universitätsstr. 1, 40225 Düsseldorf, Germany

Correspondence to: Christian Steinhäuser, PhD,
Institute of Cellular Neurosciences,
University of Bonn,
Sigmund-Freud-Str. 25,
D-53105 Bonn,
Germany
E-mail: Christian.Steinhaeuser@ukb.uni-bonn.de

Keywords: gap junction coupling; gap junction protein alpha 1; temporal lobe epilepsy; hippocampal sclerosis; inflammation

Abbreviations: EGFP = enhanced green fluorescent protein; EYFP = enhanced yellow fluorescent protein; hpi = hours post kainate injection; HS = hippocampal sclerosis; mpi = months post kainate injection; MTLE = mesial temporal lobe epilepsy; SR101 = sulforhodamine 101; TUNEL = terminal deoxynucleotidyl transferase dUTP nick end labelling

Received October 10, 2014. Revised January 12, 2015. Accepted January 13, 2015. Advance Access publication March 12, 2015

Introduction

Epilepsy is a condition of the brain that affects 1% of the population worldwide, and one-third of the patients are refractory to medical treatment. This disorder has for a long time been considered to be caused by dysfunctional neurons. Hence, search for new antiepileptic drugs has concentrated largely on compounds that affect neuronal function. As efficacy and tolerability of these drugs have not substantially improved over the past decades, and all known antiepileptic drugs merely suppress symptoms without treating the underlying disorder, new strategies in antiepileptic drug development are required (Löscher and Schmidt, 2011; Simonato *et al.*, 2012). In this context, glial cells, astrocytes in particular, have attracted increasing attention. These cells play essential roles in brain physiology: they modulate synaptic transmission and control ion homeostasis and blood–brain barrier integrity (Perea *et al.*, 2009; Halassa and Haydon, 2010). Impairment of these functions has been associated with the pathophysiology of neurological disorders, including epilepsy, yet the underlying mechanisms remain enigmatic (Seifert *et al.*, 2006, 2010). In the sclerotic hippocampus of patients with mesial temporal lobe epilepsy (MTLE-HS), glial cells lose the glutamate-metabolizing enzyme, glutamine synthetase (Eid *et al.*, 2004), and display reduced inwardly rectifying K^+ currents (Bordey and Sontheimer, 1998; Hinterkeuser *et al.*, 2000; Kivi *et al.*, 2000), which was speculated to contribute to generation and spread of seizure activity.

Astrocytes are connected by gap junction channels composed mainly of the gap junction protein alpha 1 (GJA1, connexin 43) and gap junction protein beta 6 (GJB6, connexin 30) (Nagy and Rash, 2000; Giaume *et al.*, 2010). These networks were proposed to counteract hyperactivity by facilitating extracellular K^+ and glutamate removal, thereby attenuating synaptic transmission. In mice with coupling-deficient astrocytes disturbed K^+ and glutamate clearance, spontaneous epileptiform activity and decreased seizure thresholds have been described (Wallraff *et al.*, 2006; Pannasch *et al.*, 2011). Previous studies on connexin expression in experimental epilepsy were inconsistent (Nemani and Binder, 2005; Giaume *et al.*, 2010; Steinhäuser *et al.*, 2012). Patients with pharmacoresistant MTLE-HS displayed enhanced or unchanged GJA1 immunoreactivity or transcript levels (Steinhäuser *et al.*, 2012). However, alterations in mRNA or protein levels do not necessarily correlate with functional changes. Importantly, so far functional coupling has not been investigated in human specimens.

In the present study we combined patch clamp recording, rapid glutamate application, extracellular K^+ concentration analysis, EEG and video monitoring and fate mapping analysis to ask whether impaired gap junction function might be involved in the aetiology of epilepsy. We have investigated, for the first time, coupling in astrocytes of hippocampal specimens freshly dissected from patients presenting with intractable MTLE. To decide whether the glial changes we observed in human epileptic hippocampus represent cause or effect of MTLE-HS, we developed a mouse model, unilateral intracortical kainate injection, which reproduces key features of the human condition. Our data identify astrocyte uncoupling as a key event in epileptogenesis and unravel novel targets for anti-epileptogenic therapeutic intervention.

Materials and methods

Patient data

Hippocampal specimens were obtained from 119 patients with pharmacoresistant MTLE. Histopathological evaluation revealed hippocampal sclerosis in 75 patients, characterized by severe neuronal loss in the CA1, CA3 and CA4 subregions of the hippocampus. Medication of patients with hippocampal sclerosis with the antiepileptic drug levetiracetam did not affect basic membrane properties of the glial cells analysed (resting potential, inwardly rectifying K^+ current density, membrane capacitance). Another 44 patients, suffering from lesion-associated epilepsy, showed no or only minor morphological changes (i.e. no significant hippocampal atrophy, neuronal death or granule cell dispersion, but mild to moderate astrogliosis and/or microglia activation) in the hippocampus. Clinical details of MTLE patients are shown in Supplementary Table 1. In all patients, the hippocampus was shown to be intimately involved in the generation of temporal lobe seizures by non-invasive and invasive diagnostics as described elsewhere (Elger *et al.*, 1993; Behrens *et al.*, 1994). Informed consent was obtained from all patients for additional electrophysiological evaluation. All procedures were approved by the ethics committee of Bonn University Medical Centre and conform to standards set by the Declaration of Helsinki (1989).

Preparation of human tissue

Human tissue sections were prepared as reported (Hinterkeuser *et al.*, 2000). Hippocampal specimens were cut perpendicular to the septotemporal axis into blocks of 3–4 mm using a razor blade and then slices of 200-µm thickness were cut in ice cold preparation solution containing (in mM): 87 NaCl, 2.5 KCl, 1.25 NaH_2PO_4, 25 $NaHCO_3$, 7 $MgCl_2$, 0.5 $CaCl_2$, 25 glucose, 75 sucrose, on a vibratome (Leica VT1000 S, Leica Biosystems). Subsequently, slices were stored for at least 30 min in artificial CSF containing (in mM): 126 NaCl, 3 KCl, 2 $MgSO_4$, 2 $CaCl_2$, 10 glucose, 1.25 NaH_2PO_4, 26 $NaHCO_3$. By gassing the solution with carbogen (5% CO_2/95% O_2) the pH was adjusted to 7.4. For patch-clamp analysis, slices were placed in a perfusion chamber installed on the stage of an upright microscope (Axioskop FS, Zeiss or Nikon Eclipse FN1) and fixed with a grid of nylon threads. The chamber was continuously perfused with oxygenated standard solution and drugs were added to the bath as indicated. Recordings were obtained from cells located in the hippocampal CA1 region. The selected cells were located about 30 µm underneath the surface of the slice and could be approached by

the patch pipette using water immersion optics (LUMPlanFI/IR ×60, Olympus, or CFI APO ×60-W NIR, Nikon). Positive pressure was applied to the recording pipette while the cell was approached under microscopic control. Cells were morphologically identified by use of an infrared camera (C5204, HAMAMATSU, or VX45, Optronis).

Animals

Maintenance and handling of animals (specific pathogen-free; House of Experimental Therapy, UKB Bonn) was according to local government regulations. Experiments have been approved by the State Office of North Rhine-Westphalia, Department of Nature, Environment and Consumerism (approval number 84-02.04.2012.A212). All measures were taken to minimize the number of animals used. If not stated otherwise, transgenic mice with human *GFAP* promoter-controlled expression of EGFP (hGFAP/EGFP mice, Nolte *et al.*, 2001) were used. In addition, some experiments were performed with Toll-like receptor 4 (TLR4) knockout mice, which carry a deletion in the *Tlr4* gene that results in the absence of both mRNA and protein (C57Bl/10ScNJ mice; The Jackson Laboratory). Male mice aged 3–6 months were used unless stated otherwise. For fate mapping, ROSY reporter mice [*Gt(ROSA)26Sor*$^{tm1(EYFP)Cos}$], which contain a floxed 'stop' sequence followed by the enhanced yellow fluorescent protein (EYFP) gene inserted into the *ROSA26* locus (Srinivas *et al.*, 2001), were bred with a mouse expressing tamoxifen-inducible Cre recombinase (Cre-ERT) under control of *Gja1* promoter [*Gja1*$^{tm5(cre/ERT)Kwi}$] mice (Eckardt *et al.*, 2004). To induce recombination in the double transgenic offspring, 1 mg tamoxifen (Sigma) was injected intraperitoneally twice a day for five consecutive days. Tamoxifen was dissolved in 50 µl sunflower oil (Fluka) containing 10% ethanol per mg tamoxifen. Mice were injected at 8–9 weeks of age and subjected to the kainate model of epilepsy (see below) 4–5 weeks after the first injection of tamoxifen.

Preparation of mouse brain slices, solutions and electrodes

Mice were anaesthetized (between 10–11 am) with 50% CO_2, decapitated, the brains were quickly removed and 200-µm thick coronal slices were cut on a vibratome (VT1000S, Leica). During cutting, brains were submerged in ice-cold oxygenated solution containing (in mM): 150 NaCl, 5 KCl, 2 $MgSO_4$, 1 Na-pyruvate, 10 glucose, 10 HEPES, pH 7.4. The standard bath solution contained (in mM): 150 NaCl, 5 KCl, 2 $MgCl_2$, 2 $CaCl_2$, 10 HEPES and 10 glucose (320 mOsm; pH 7.4). For uncaging experiments, 5 mM TEA, 4 mM 4-AP, 2 mM $BaCl_2$, 0.1 mM $CdCl_2$ and 1 µM tetrodotoxin were added. Gap junctional coupling analyses were performed in artificial CSF. The pipette solution contained (in mM): 130 K-gluconate, 1 $MgCl_2$, 3 Na_2-ATP, 20 HEPES and 10 EGTA (280 mOsm; pH 7.2). For gap junction coupling analysis, biocytin (Sigma) was added to the internal solution (0.5%). Experiments on outside-out patches were performed with a pipette solution containing (in mM): 130 KSCN, 2 $MgCl_2$, 0.5 $CaCl_2$, 3 Na_2-ATP, 10 HEPES and 5 BAPTA to facilitate detection of uptake currents. Recording pipettes were fabricated from borosilicate capillaries (Hilgenberg).

Electrophysiology and drug application

Membrane currents were measured with the patch-clamp technique in the whole-cell and outside-out patch configurations. Current signals were amplified (EPC 8 or EPC 9 amplifier; HEKA), filtered at 3 or 10 kHz, and sampled at 10 or 30 kHz. Online analysis was performed with 'TIDA for Windows' acquisition and analysis program (HEKA). The resistance of the patch pipettes was 3–6 MΩ. Capacitance and series resistance compensation (up to 50%) were used to improve voltage clamp control. Voltages were not compensated for liquid junction potentials. Recordings were performed at room temperature (20–22°C).

For fast application of glutamate to outside-out patches, a theta glass tube was positioned right-angled with the patch pipette and driven by a piezo translator (P-245.50, Physik Instrumente). The flow rate through the two barrels was adjusted with a syringe pump (solution exchange ~300 µs; Matthias *et al.*, 2003). In some experiments glutamate was applied through flash photolysis. 4-methoxy-7-nitroindolinyl-caged-L-glutamate (10 mM, Toc ris) was liberated by a Xenon flash-lamp (JML-C2; Rapp OptoElectronic). Tracer coupling analyses were performed as described (Wallraff *et al.*, 2004).

$[K^+]_o$ measurements and imaging

Combined two-photon excitation fluorescence imaging and electrophysiological recordings from astrocytes were performed as reported (Henneberger and Rusakov, 2012). Briefly, acute 300-µm thick coronal hippocampal slices were prepared 4 h post kainate injection (hpi) (Supplementary material) in a slicing solution containing (in mM) 105 sucrose, 60 NaCl, 2.5 KCl, 7 $MgCl_2$, 0.5 $CaCl_2$, 1.25 NaH_2PO_4, 1.3 ascorbic acid, 3 sodium pyruvate, 26 $NaHCO_3$, 10 glucose. Slices were allowed to recover at 34°C for 15 min before storage in artificial CSF at 34°C for 45 min and room temperature afterwards. CA1 stratum radiatum astrocytes were patched using the K-gluconate-based pipette solution supplemented with 0.04 mM Alexa Fluor® 594 hydrazide and identified by their low input resistance, low membrane potential, 'ohmic' responses to current injections and characteristic morphology (Steinhäuser *et al.*, 1994; Henneberger and Rusakov, 2012). Schaffer collaterals were stimulated using bipolar concentric electrodes (single pulses, 100 µs, 160 µA, at least 10 trials). Voltage responses were recorded from astrocytes held in current clamp (Multiclamp 700B, Molecular Devices). The access resistance was continuously monitored, and recordings were rejected if the access resistance exceeded 15 MΩ or if it changed more than 30%. Astrocyte voltage responses to axonal stimulation in the absence of synaptic transmission are composed of the axonal fibre volley, a quickly decaying transporter component (decay time constant <15 ms) followed by a long-lasting depolarization due to an increase of the extracellular K^+ concentration ($[K^+]_o$) (Bergles and Jahr, 1997; Diamond, 2005; Henneberger and Rusakov, 2012). The latter was analysed 50–60 ms after the stimulus (ΔV_K, average voltage relative to prestimulus baseline, Fig. 4) and normalized to the fibre volley amplitude to account for varying axonal stimulation efficacy between recordings. Synaptic transmission was

blocked to avoid potential bias due to kainate-induced alterations of synaptic transmission and excitability (50 μM APV, 10 μM NBQX, 100 μM picrotoxin and 5 μM CGP52432). In a subset of recordings, extracellular field potentials were recorded in parallel to astrocyte voltage responses in the immediate vicinity of the astrocyte. Fibre volley amplitudes recorded extracellularly and from astrocytes were strongly correlated ($R = 0.923$, $n = 12$). In contrast to astrocyte recordings of ΔV_K (on average 0.193 ± 0.03 mV, $n = 12$) paired extracellular recordings did not display a long-lasting voltage shift (0.0002 ± 0.0005 mV, $n = 12$). Image stacks of cells filled with Alexa Fluor® 594 and dye escape into gap junction-coupled astrocytes were acquired 25–30 min after break-in using two-photon excitation fluorescence imaging (Olympus MPE, 25× objective, NA 1.05, Coherent Vision S tuned to 800 nm, power at objective <6 mW) and analysed offline.

To test whether 4 hpi the astrocytic membrane was still dominated by a high K^+ resting conductance, input resistance and resting potential of CA1 stratum radiatum astrocytes on the contra- and ipsilateral sides (underneath the injection site) were compared. No significant difference was found for the input resistance (contralateral 2.1 ± 1.1 MΩ, $n = 33$; ipsilateral 2.6 ± 1.2 MΩ, $n = 31$) while the resting potential was slightly depolarized ipsilaterally (contralateral -77 ± 3.9 mV, $n = 33$; ipsilateral -73.5 ± 4.2 mV, $n = 31$). We conclude that at this early time point after kainate injection, the dominating resting K^+ permeability of the astrocytic membrane is still preserved.

Immunohistochemistry

The surgically resected hippocampal blocks of 3–4 mm thickness (see Supplementary material) were incubated in 2–4% paraformaldehyde for 24–30 h, washed in phosphate buffered saline (PBS) and sectioned by a vibratome (Leica VT1200S) at 40 μm. After permeabilization and blocking (1 h) with 0.5% Triton™ X-100 and 10% normal goat serum (NGS) in PBS, the sections were incubated overnight (4°C) in 2% NGS in PBS containing 0.1% Triton™ X-100 containing primary antibodies. The sections were washed in PBS and incubated in secondary antibodies coupled to Alexa Fluor® 488 or Alexa Fluor® 594 (1:500, Invitrogen) for 1 h at room temperature in 2% NGS in PBS. After several washing steps nuclei were stained with Draq5 (1:1000; Biostatus) in PBS for 10 min. The following primary antibodies were used: rabbit anti-PDGFRA (sc-338; 1:1500; Santa Cruz Biotechnology), mouse anti-GFAP (MAB 360; 1:400; Millipore), mouse anti-CSPG4 (MAB2029; 1:350; Millipore), rabbit anti-S100B (ab41548; 1:3000; Abcam) and mouse anti-S100B (ab16959; 1:200; Abcam). Images were obtained using a confocal laser scanning microscope (TCS NT, Leica Lasertechnik). To compare cell densities or co-expression of cell markers in MTLE-HS and non-hippocampal sclerosis human hippocampal tissue, cells were counted in a volume of $250 \times 250 \times 10\ \mu m^3$.

Mice were anaesthetized and intracardially perfused with PBS followed by 4% paraformaldehyde solution. Brains were postfixed, removed and cut on a VT1200S (Leica) into coronal slices (40 μm). Slices were blocked for 2–4 h at room temperature in PBS containing 2% Triton™ X-100 and 10% NGS. First antibody was incubated in PBS containing 0.1% Triton™ X-100 and 2% NGS at 4°C overnight. The following primary antibodies were used: rabbit anti-CSPG4 (anti-NG2; AB5320, 1:100, Millipore), rabbit anti-AIF1 (anti-Iba1; 019-19741, 1:400, Wako), mouse anti-NeuN (MAB377, 1:200, Chemicon), mouse anti-GFAP (MAB 360, 1:400, Millipore), rabbit anti-GFAP (Z0334, 1:400, Dako), rabbit anti-GFP (132002, 1:1000, Synaptic Systems), mouse anti-GFP (A11120, 1:500, Invitrogen). The next day, slices were washed three times in PBS and incubated with the appropriate goat polyclonal secondary antibodies conjugated to Alexa Fluor® 488 and Alexa Fluor® 594 (1:500; Invitrogen). Slices were washed three times and incubated with Draq5 (1:1000, Biostatus) for nuclear staining, washed again and mounted on coverslips with Aquapolymount (Polysciences). Terminal deoxynucleotidyl transferase dUTP nick end labeling (TUNEL) was performed with the Click-iT TUNEL Alexa Fluor® Imaging Assay (Invitrogen) according to the manufacturer's instructions. Fluoro-jade® C/DAPI double staining was performed using Biosensis® Ready-to-Dilute (RTD)™ kit (TR-100-FJ, Biosensis) following the instructions of the manufacturer. For sulforhodamine 101 (SR101) labelling (Nimmerjahn *et al.*, 2004), slices were incubated in SR101 (1 μM, Sigma) in oxygenated artificial CSF for 20 min at 35°C. Biocytin was visualized with streptavidin-Cy3 (1:300, Sigma), -Cy2 (1:100, Sigma) or -Cy5 (1:200, Jackson ImmunoResearch). Images were acquired at 1–2 μm z steps using a fluorescence microscope (Axiophot, Zeiss) and MetaVue software, or employing confocal microscopy (TCS NT, Leica).

To minimize subjective bias, cell counting and assessment of co-staining was always performed by two different persons blinded to the respective experimental condition.

Immunoblotting

Western blot analysis of hippocampal protein extracts prepared from 8–10 week old hGFAP/EGFP mice were performed as previously described (Zhang *et al.*, 2013). For immunodetection polyclonal rabbit anti-GJB6 (1: 250; Invitrogen), anti-GJA1 antibodies (1: 5000; Sigma) and monoclonal mouse anti-tubulin antibodies (1:10 000; Sigma) were used. Secondary antibodies used: goat-anti-mouse horseradish peroxidase conjugate (1:10 000, GE Healthcare) and goat-anti-rabbit horseradish peroxidase conjugate (1:10 000, GE Healthcare). For visualisation of horseradish peroxidase, the West Dura substrate (Pierce) was used and chemiluminescence was detected with the Gene Gnome digital documentation system (Synoptics). GJB6 and GJA1 protein expression levels were normalized to tubulin.

Data analysis

The membrane capacitance was estimated from the current transients evoked by a 10 mV test pulse depolarizing the cells to −60 mV (sampling rate 30 kHz, filter 10 kHz). Because the inward rectifier is still active in this voltage range, we did not compensate for resting conductance or leakage (Akopian *et al.*, 1997). Data are given as mean ± standard deviation (SD). Differences between data were tested for significance using the Student's *t*-test, ANOVA with *post hoc* test or χ^2 test as appropriate. The level of significance was set at $P < 0.05$.

Results

Glutamate sensitivity and coupling in glial cells of non-sclerotic human hippocampus

Whole-cell recordings were obtained from glial cells in the CA1 stratum radiatum of 'control-like', i.e. non-sclerotic human hippocampus (non-HS; 44 specimens). Based on morphological and electrophysiological criteria, glial cells with complex ($n = 147$) and passive currents ($n = 134$) were distinguished (Fig. 1A, C, left traces, H) (Hinterkeuser *et al.*, 2000), resembling NG2 cells (previously termed complex or GluR cells) (Bergles *et al.*, 2010) and astrocytes in murine hippocampus. In the latter, NG2 cells and astrocytes differ in their glutamate sensitivity and gap junction coupling (Matthias *et al.*, 2003; Wallraff *et al.*, 2004). We tested whether human glial cells share similar segregated glutamate sensitivity. Outside-out patches were excised from the soma of astrocytes and glutamate (1 mM) was rapidly applied. At negative voltages, transient inward currents were activated (17 ± 11 pA; time constant 3.9 ± 1.3 ms; -70 mV; $n = 9$ cells, seven patients) while no outward currents occurred at positive potentials (up to $+50$ mV) (Fig. 1A). Inward currents were completely blocked by DL-TBOA (100 µM, $n = 3$), but insensitive to NBQX (20 µM, $n = 2$, not shown), indicating that they were due to glutamate uptake. The glutamate sensitivity of human NG2 cells was investigated through flash photolysis (caged glutamate, 10 mM) or fast glutamate (1 mM) application to excised patches ($n = 8$ cells, six patients). Both methods revealed rapidly decaying currents (reversal at 12.7 ± 6 mV; Fig. 1C), which were blocked by kynurenic acid (5 mM) or NBQX (20 µM, not shown; see Seifert *et al.*, 2004). Thus, NG2 cells expressed ionotropic receptors but not glutamate transporters. Next, gap junction coupling was investigated with biocytin filling. Astrocytes ($n = 20$ cells, eight patients) were always coupled (Fig. 1B; tracer spread to 94 ± 84 cells) while NG2 cells ($n = 10$ cells, seven patients) lacked coupling (Fig. 1D). Double-labelling revealed that the majority (98.6%) of human GFAP-positive cells co-expressed S100B [Supplementary Fig. 1A(2)] but not PDGFRA, a marker of NG2 cells [Supplementary Fig. 1A(1)]. PDGFRA-positive cells consistently expressed S100B [Supplementary Fig. 1A(3)] and CSPG4 (NG2, $n = 3$ slices, three patients, data not shown). Thus, human NG2 cells and astrocytes displayed the same properties as their counterparts in rodent brain.

Lack of *bona fide* astrocytes and gap junction coupling in human MTLE-HS

We next tested if the properties of glial cells were changed in patients with MTLE-HE (75 specimens). In spite of trying to select astrocytes, almost all cells (98%) displayed complex currents ($P < 0.0001$, $n = 325$). As reported by Hinterkeuser *et al.* (2000), depolarization through current injections (up to $+10$ mV) never elicited action potentials in these cells ($n = 11$, not shown). Fast application of glutamate (1 mM) to outside-out patches always evoked receptor-mediated responses ($n = 13$ cells, seven patients) (Fig. 1E, G and H). However, when NBQX (20 µM) was co-applied ($n = 6$) the glutamate-evoked responses with almost linear current/voltage relationships (reversal potential 10 ± 1.1 mV, Fig. 1E) were inhibited only partially in 50% of the cells (to 38.8 ± 2.8%, V = -130 mV, Fig. 1G), suggesting co-expression of ionotropic glutamate receptors and glutamate transporters. This has been observed neither in glial cells from non-hippocampal sclerosis specimens (Fig. 1) nor mouse hippocampus (Matthias *et al.*, 2003). Membrane potential, input resistance and capacitance of the two glial cell types with distinct glutamate sensitivity were not different. Biocytin loaded into individual glial cells in the CA1 region of MTLE-HS specimens never spread into neighbouring cells ($n = 25$ cells, 16 patients, Fig. 1F). Immunohistochemistry revealed pronounced, diffuse GFAP-immunoreactivity [Supplementary Fig. 1B(1 and 2)]. Individual cells were only detectable by co-staining with S100B [Supplementary Fig. 1B(2)]. GFAP never co-localized with PDGFRA [Supplementary Fig. 1B(1)], ruling out ectopic expression of GFAP in NG2 cells in human MTLE-HS. Similar to non-hippocampal sclerosis specimens, PDGFRA-positive cells co-expressed S100B [Supplementary Fig. 1B(3)] and CSPG4 (NG2, four slices, three patients, data not shown).

Together, we concluded that tissue from patients with MTLE-HS was devoid of *bona fide* astrocytes, and contained glial cells with abnormal functional properties.

The unilateral intracortical kainate injection model reproduces key aspects of human MTLE-HS

Loss of astrocyte gap junction coupling as observed in human MTLE-HS might entail hyperactivity due to impaired K^+ and neurotransmitter homeostasis. As freshly-dissected human brain specimens are only available from the chronic state of the disorder, an animal model was established to investigate whether reduced coupling contributes to epileptogenesis. We used unilateral intracortical kainate injections in hGFAP/EGFP mice, an approach that is based upon the intrahippocampal kainate model (Suzuki *et al.*, 1995; Bouilleret *et al.*, 1999; Riban *et al.*, 2002) but avoids damage to the CA1 region by the injection needle (Supplementary material and Supplementary Fig. 2). This model reliably reproduces key morphological and functional features of chronic human MTLE-HS (Supplementary Figs 3–6). After kainate injection, mice developed status epilepticus followed by a latent period and generation of spontaneous recurrent seizures. Seizures occurred bilaterally and recruited the hippocampus

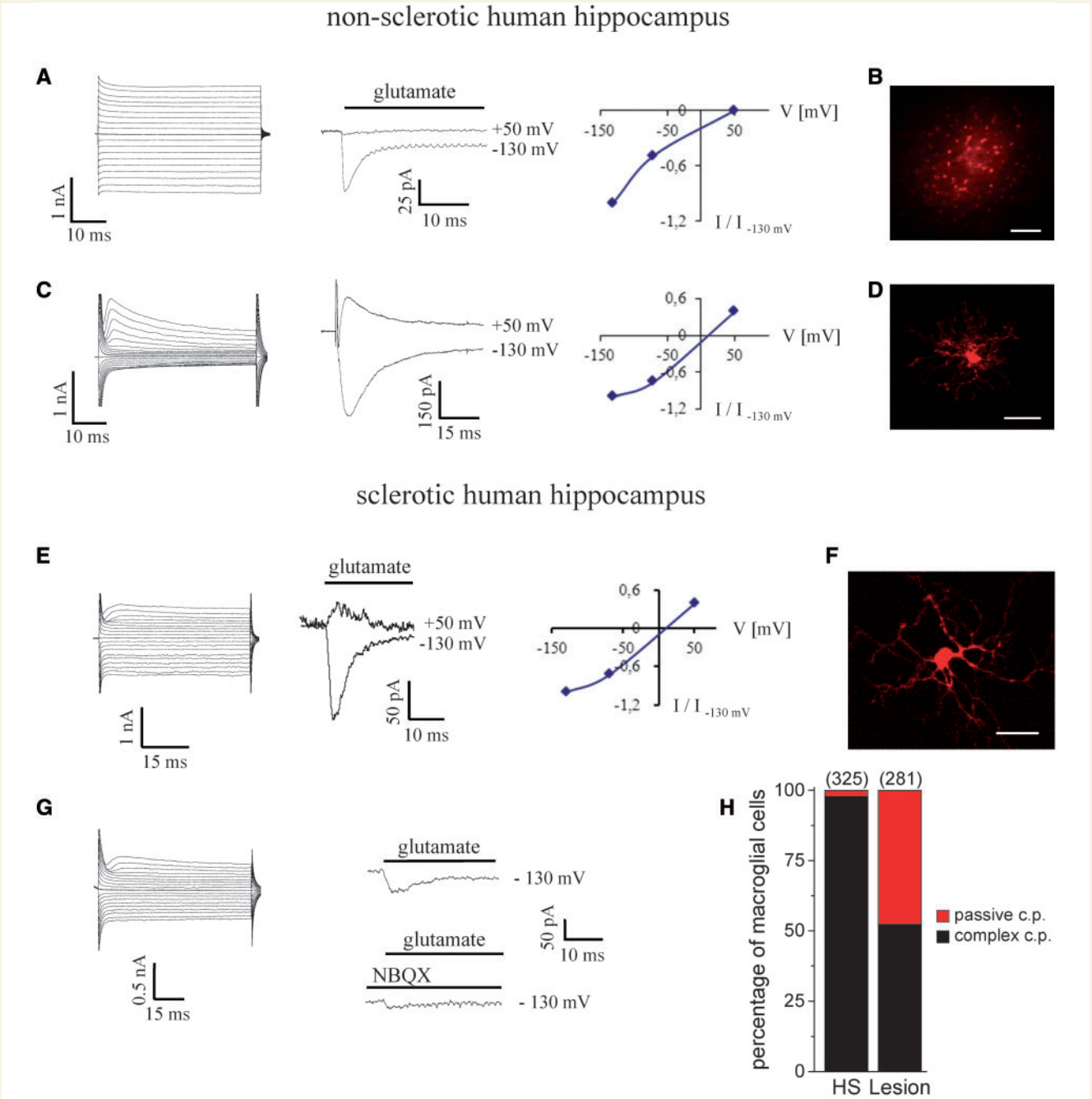

Figure 1 Characterization of astrocytes and NG2 cells in non-sclerotic and sclerotic human hippocampus. (**A**) The whole-cell current pattern of an astrocyte (left; 50 ms voltage steps ranging from −160 to +20 mV; 10 mV increments; V_{hold} = −80 mV) was dominated by a passive resting conductance. Rapid application of glutamate to an outside-out patch failed to induce outward currents at positive voltages (*middle* and *right*), indicating the absence of ionotropic receptors. The inward currents were due to glutamate uptake. (**B**) Gap junction coupling between hippocampal astrocytes visualized by diffusion of biocytin from a single cell, filled with the tracer through the patch pipette during a 20 min whole-cell recording. Scale bar = 100 μm. (**C**) Typical whole-cell current pattern of an NG2 cell (*left*). De- and hyperpolarization activated time- and voltage-dependent out- and inward currents. Flash photolysis of caged glutamate activated currents with a linear current/voltage plot (*middle* and *right*), indicating the expression of ionotropic receptors. (**D**) Biocytin filling of NG2 cells revealed lack of tracer coupling. Scale bar = 25 μm. (**E**) Complex current pattern resembling an NG2 cell in human hippocampal sclerosis (*left*). Application of glutamate to an outside-out patch excised from the soma demonstrates expression of ionotropic glutamate receptors with a linear current/voltage curve (*middle* and *right*). (**F**) Intercellular diffusion of biocytin was never observed in hippocampal sclerosis. Scale bar = 25 μm. (**G**) Some of these cells co-expressed ionotropic glutamate receptors and glutamate transporters, as revealed by the incomplete block of inward currents by NBQX. (**H**) Almost complete loss of cells with passive current pattern was noted in the hippocampus of patients with MTLE-HS. Number of investigated cells in brackets; c.p. = current pattern.

(Supplementary Fig. 4). Three months post injection (mpi), strong GFAP immunoreactivity was found in the sclerotic CA1 region. Nine months after status epilepticus, the diffuse GFAP staining pattern lacked clearly discernible cellular structures, similar to human MTLE-HS (Supplementary Fig. 6A). As in human hippocampal sclerosis, GFAP did not co-localize with markers for NG2 cells (Supplementary Fig. 6B).

Biocytin filling was performed in non-sclerotic and sclerotic hippocampal segments of the injected and contralateral hemisphere. Sclerotic slices displayed complete loss of CA1 pyramidal neurons, hippocampal atrophy, gliosis, and granule cell dispersion (Supplementary Fig. 5A). Astrocytes were identified by their morphology and passive membrane currents. Three and 6 months after status epilepticus, cells matching the above criteria could still be found. However, these cells lacked coupling (Fig. 2A and B; $P < 0.0001$ for both time points). Nine months after status epilepticus, cells with passive currents were no longer detected in the sclerotic region ($P = 0.019$). In contrast, in non-sclerotic hippocampal slices of the injected hemisphere and slices from the contralateral hippocampus, astrocytes displayed abundant coupling at all time points investigated (Fig. 2B).

When selecting cells under the microscope for patch clamp analysis, one might argue that the investigator simply has overlooked astrocytes in the sclerotic tissue. To avoid such a potential bias and confirm loss of *bona fide* astrocytes in MTLE-HS with an alternative approach, we performed SR101 labelling (Nimmerjahn *et al.*, 2004; Kafitz *et al.*, 2008). At 9 mpi, SR101 failed to label cells in the sclerotic CA1 region whereas abundant SR101 labelling was found in non- or weakly-sclerotic slices from the ventral part of the injected hippocampus, and in slices from the contralateral hippocampus (Fig. 2C).

To test whether dysfunctional astrocytes contribute to epileptogenesis, we investigated coupling 4 h, 24 h and 4–5 days post injection (Fig. 3). EEG analysis was used to exclude onset of spontaneous seizures before coupling analysis. At all three time points we observed decreased tracer spread ipsilaterally compared to the contralateral side (Fig. 3C). TUNEL staining identified apoptotic neuronal death 6 hpi whereas no TUNEL-positive cells were seen in the pyramidal layer 4 hpi (Fig. 3B), a time point when coupling was already dramatically decreased. Using fluoro-jade C, a highly specific marker for neurodegeneration, revealed faintly positive cells at 4 hpi (Supplementary Fig. 7). Sham injection did not affect coupling (Fig. 3C). Thus, decreased astrocyte coupling precedes apoptotic cell death and the onset of spontaneous seizure activity, suggesting its critical involvement in epileptogenesis.

To test whether decreased gap junction coupling 4 hpi impaired K^+ clearance, we exploited the high sensitivity of the astrocyte membrane potential to changes of $[K^+]_o$ (Fig. 3D–G) (Meeks and Mennerick, 2007; Djukic *et al.*, 2007). Filling cells with Alexa Fluor® 594 confirmed decreased gap junction coupling as seen with biocytin (Fig. 3C and E). Stimulation of Schaffer collaterals was followed by a small, long-lasting astroglial depolarisation (ΔV_K) even in the absence of synaptic transmission, reflecting an increase in $[K^+]_o$ (Bergles and Jahr, 1997; Henneberger and Rusakov, 2012; Liotta *et al.*, 2012). We compared ΔV_K (normalized to the fibre volley) in the presence and absence of the gap junction blocker carbenoxolone (50 µM). In contralateral tissue we found a 59% increase of ΔV_K in carbenoxelone (Fig. 3F and G), but importantly, ΔV_K recorded ipsilaterally was rendered insensitive to carbenoxolone. These findings imply that the epileptic condition severely impaired the ability of astrocytes to regulate $[K^+]_o$, favouring hyperexcitability and epileptogenesis. When comparing ΔV_K ipsi- and contralaterally it should be considered that according to the Goldman equation, the same depolarization requires increasingly larger $[K^+]_o$ increases as the resting potential becomes more positive.

Astrocytes acquire an abnormal phenotype in chronic epilepsy

To investigate the fate of astrocytes in epilepsy, we used mice with inducible EYFP expression in astrocytes. Cre-mediated recombination of the EYFP reporter was induced by tamoxifen injection, resulting in permanent labelling of astrocytes. This approach labels 70–80% of GFAP-positive astrocytes in the CA1 region (Gosejacob *et al.*, 2011). In line with these previous findings, 8 weeks and 6 months after tamoxifen all fluorescent cells investigated ($n = 63$ cells, six animals) displayed passive current patterns and coupling (Supplementary Fig. 8A). To determine whether trans-differentiation into another cell type accounted for the loss of astrocytes during epileptogenesis, kainate was injected 4 weeks after tamoxifen. Patch-clamp and gap junction coupling analyses of fluorescent cells in the CA1 stratum radiatum were performed 4–5 days post injection, 3 mpi and 6 mpi (Fig. 4A). Four to 5 days post injection, all fluorescent cells displayed passive currents and coupling. However, biocytin-spread ipsilaterally was decreased by 50% (Fig. 4C), confirming data obtained from hGFAP/EGFP mice (Fig. 3C). Three and 6 mpi, an increasing number of fluorescent cells in sclerotic tissue showed current patterns atypical of astrocytes (input resistance > 40 MΩ and/or voltage- and time-dependent currents) and lacked coupling (Fig. 4B–D; Supplementary Fig. 8B). Immunohistochemistry 3 and 6 mpi revealed that all EYFP-positive cells expressed GFAP but not NG2 (Supplementary Fig. 8C). These data demonstrate that at later stages of epileptogenesis, astrocytes acquire an atypical phenotype. To test whether astrocyte death added to the loss of *bona fide* astrocytes in chronic MTLE-HS, TUNEL/GFAP/Draq5 triple staining was performed 1 and 4–5 days post injection, 3 and 6 mpi. As expected (Theofilas *et al.*, 2009), at 1 and 4–5 days post injection

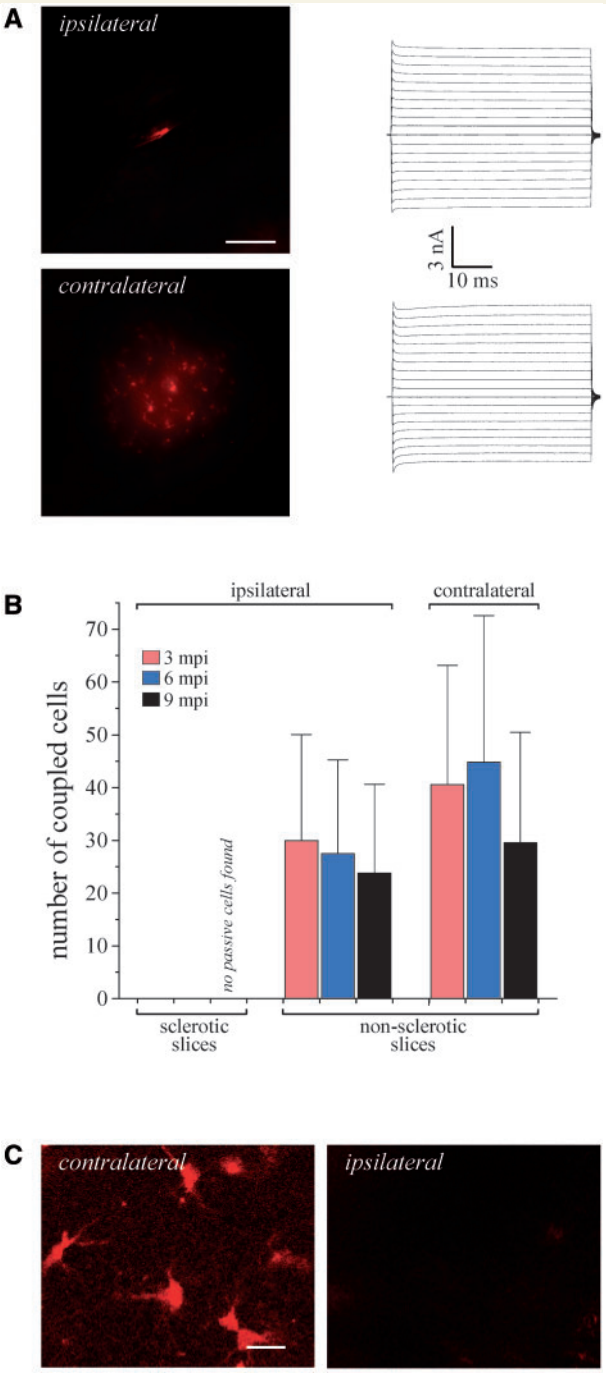

Figure 2 Loss of *bona fide* astrocytes and gap junction coupling in the hippocampus of kainate-injected mice. (**A**) Representative example showing abolished tracer coupling in sclerotic slices obtained from epileptic mice 3 mpi (*top left*). In contrast, in the contralateral hippocampus astrocytes displayed abundant gap junction coupling, resembling control conditions (*bottom left*). Scale bar = 100 μm. Whole-cell currents of the filled cells were elicited as described in the legend to Fig. 1A (*right*). (**B**) Summary of tracer coupling experiments. The extent of intercellular biocytin diffusion was compared in sclerotic and non-sclerotic slices of the injected hemisphere, and in slices from the contralateral hippocampus. Three and 6 mpi, no spread of biocytin could be detected in sclerotic slices (3 months: $n = 12$ biocytin-filled passive cells from six animals; 6 months: $n = 6$ filled passive cells, three animals). Astrocytes were still coupled in non-sclerotic hippocampal slices of the injected hemisphere (3 months: 30 ± 20.1 coupled cells, $n = 11$ slices, six animals; 6 months: 27.5 ± 17.8 coupled cells, $n = 10$ slices, five animals) and slices obtained from the contralateral hippocampus (3 months: 40.6 ± 22.5 coupled cells, $n = 10$ slices, six animals; 6 months: 44.9 ± 27.7 coupled cells, $n = 11$ slices, three animals). Nine months after status epilepticus, complete loss of cells with passive current pattern was observed in sclerotic segments of the hippocampus ($n = 18$ screened slices, six animals) whereas in non-sclerotic hippocampal slices ipsilateral to the injection, and in the contralateral hippocampus, astrocytes coupled to 23.8 ± 16.8 ($n = 13$ slices, five animals) and 29.6 ± 21 ($n = 18$ slices, five animals) cells, respectively. Gap junction coupling in non-sclerotic ipsilateral slices did not differ from the contralateral side. (**C**) Loss of SR101 uptake by astrocytes in the sclerotic hippocampus. Incubation with SR101 of slices from epileptic mice 9 mpi resulted in astrocytic labelling in the contralateral CA1 region. In the ipsilateral hippocampus, no labelled cells were detected ($n = 3$ slices, three animals). Scale bar = 15 μm.

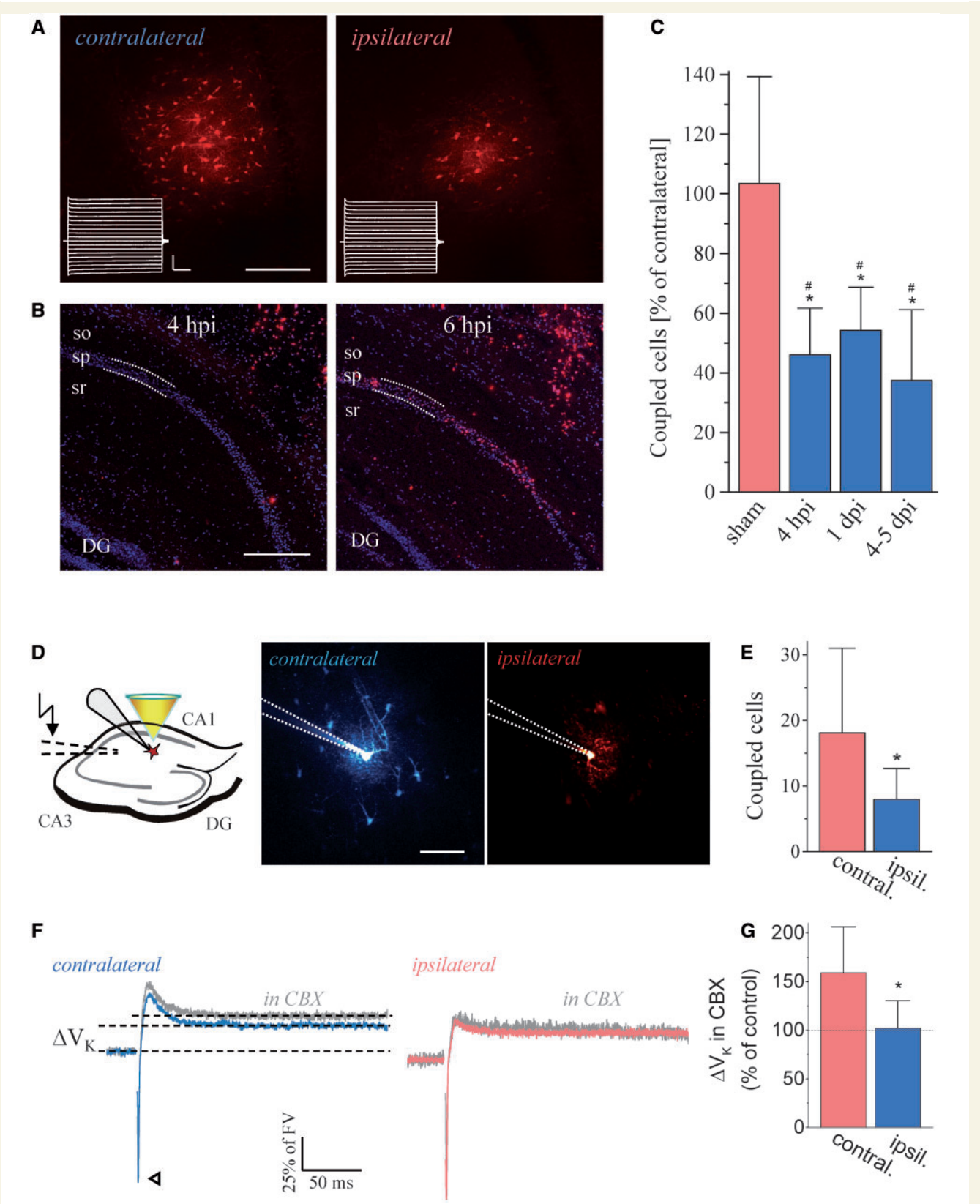

Figure 3 Decreased tracer coupling and impaired K^+ clearance in the latent period after kainate injection. (**A**) Representative example showing reduced tracer coupling in the ipsilateral hippocampus 4 hpi. Scale bar = 100 μm. Insets show current responses of the filled cells (stimulus protocol as in Fig. 1A; horizontal bar, 10 ms; vertical bar, 2.5 nA). (**B**) Ipsilateral TUNEL performed 4 and 6 hpi. No TUNEL-positive cells could be detected in the pyramidal layer 4 hpi (n = 7 slices from three animals), whereas abundant staining of pyramidal neurons was found underneath the injection site 6 hpi (n = 7 slices from three animals). sr = stratum radiatum; sp = stratum pyramidale; so = stratum oriens. Scale

(continued)

many CA1 and CA3 pyramidal neurons were TUNEL-positive, as opposed to GFAP-positive cells, which were TUNEL-negative (1 day post injection: $n = 6$ slices from two animals; 4–5 days post injection: $n = 12$ slices from three animals). Three and 6 mpi, TUNEL-labelling was absent in the sclerotic and non-sclerotic parts of the ipsilateral hippocampus (3 mpi: $n = 10$ slices from four animals; 6 mpi: $n = 21$ slices from three animals) (Fig. 4E). Thus, it is unlikely that the loss of astrocytes in chronic MTLE-HS is due to apoptotic cell death.

Cytokines induce uncoupling of hippocampal astrocytes

Seizures induce high levels of inflammatory cytokines, including interleukin 1 beta (IL1B) and tumor necrosis factor (TNF; Vezzani *et al.*, 2008), an effect that has been ascribed to release of damage associated molecular pattern molecules and activation of TLR4 (Maroso *et al.*, 2010). Pro-inflammatory cytokines inhibit astrocyte gap junction coupling in cell culture (Meme *et al.*, 2006). To explore whether TLR4 is involved in seizure-induced astrocytic uncoupling *in vivo*, kainate was intracortically injected into TLR4 knockout mice, and tracer coupling was quantified at 1 day post injection. During status epilepticus, wild-type and TLR4 knockout mice spent the same time in ictal activity (53.5 ± 19 min versus 47.5 ± 12.1 min, $n = 3$, $P = 0.64$). Remarkably, tracer spread ipsi- and contralaterally was not different in kainate-injected TLR4 knockout mice (Fig. 5A). To directly assess the effect of cytokines on gap junction coupling, hippocampal slices from hGFAP/EGFP mice were incubated (3–4.5 h) in IL1B, IL1B + TNF (10 ng/ml each) or lipopolysaccharide (1 μg/ml) (Lee *et al.*, 1993). Gap junction coupling was assessed in astrocytes of the CA1 stratum radiatum by biocytin filling. All conditions produced a significant decrease in gap junction coupling, which could be prevented by co-application of dibutyryl cyclic AMP (100 μM) (Fig. 5B). Next we assessed the effect of lipopolysaccharide in control mice *in vivo* through i.p. injection (5 mg/kg). At 5 days post injection, biocytin filling revealed a significant reduction of gap junction coupling (Fig. 5C). Western blot analysis performed at this time point disclosed a significant reduction of hippocampal GJA1 (to 59.2 ± 2.6%, $n = 3$, $P < 0.0001$) but unchanged GJB6 ($n = 3$, $P = 0.3$) protein levels (data not shown). Cell culture studies indicated that pro-inflammatory mediator-induced reduction of GJA1 expression and astrocytic coupling can be rescued with levetiracetam (Haghikia *et al.*, 2008; Stienen *et al.*, 2011). Therefore, we tested whether this antiepileptic drug can rescue lipopolysaccharide-induced inhibition of gap junction coupling *in vivo*. Levetiracetam was administered i.p. twice daily (150 mg/kg) for 5 days (first levetiracetam injection 6 h post lipopolysaccharide). Intriguingly, this treatment fully prevented the uncoupling effect of lipopolysaccharide (Fig. 5C).

Discussion

We performed, for the first time, coupling analyses in astrocytes of human specimens, and report an unexpected, complete lack of glial gap junction coupling and *bona fide* astrocytes in the sclerotic hippocampus of patients with MTLE-HS. Using an epilepsy mouse model reproducing key features of chronic human MTLE-HS, we demonstrate that impairment of astrocyte coupling starts very early, within 4 h after status epilepticus, and is probably mediated by hyperactivity-induced release of pro-inflammatory cytokines. Thus, astrocyte uncoupling represents a crucial event in epileptogenesis and identifies a promising new target for the development of antiepileptic drugs.

Figure 3 Continued

bar = 250 μm. (**C**) Summary of astrocytic gap junction coupling in dorsal slices of the ipsilateral hippocampus, expressed as percentage of the number on the contralateral side. Ipsi- and contralateral measurements were always conducted in the same slice. Mice, which had experienced seizures, were excluded from the study. In the ipsilateral hippocampus, astrocytic gap junction coupling was significantly reduced at each time point investigated (4 hpi: 55.2 ± 31.2 versus 119 ± 47.6 coupled cells, $P = 0.01$; $n = 12$ slices from eight animals; 1 day post injection: 53.8 ± 11.7 versus 102.6 ± 21.8 coupled cells, $P = 0.004$; $n = 10$ slices from five animals; 4–5 days post injection: 28 ± 18.2 versus 79.6 ± 27.9 coupled cells, $P = 0.001$; $n = 18$ slices from eight animals). Sham injection did not alter gap junction coupling (99.9 ± 37.6 versus 96.7 ± 30.7 coupled cells, $P = 0.6$; $n = 11$ slices from six animals). (**D**, *left*) To investigate the dependence of K^+ clearance on gap junction coupling, astrocytes were patched and held in the current clamp mode. $[K^+]_o$ increases were induced by Schaffer collateral stimulation (dashed lines). Cells were visualized by two-photon excitation fluorescence microscopy (middle and right panel, patch pipette indicated by dotted lines; Scale bar = 50 μm). Note the prominent dye coupling (Alexa Fluor® 594) to neighbouring astrocytes in control (*middle*) and reduced gap junction coupling ipsilaterally (*right*). (**E**) Quantification of dye coupling (contralateral, 18.1 ± 12.8 coupled cells; ipsilateral, 8 ± 4.8 coupled cells, $P = 0.032$, $n = 9$ and 10 slices, five and six animals, respectively). (**F** and **G**) The long-lasting, largely K^+-dependent component of astrocyte voltage responses to stimulation (ΔV_K, dotted lines) was analysed without (blue and red traces) and with (grey traces) the gap junction blocker carbenoxolone (CBX, 50 μM) present, and normalized to the fibre volley (arrowhead, synaptic transmission blocked, stimulus artefacts removed for clarity). On the contralateral side, responses were significantly larger in carbenoxolone-treated compared to untreated slices (artificial CSF, 0.187 ± 0.091, $n = 14$ cells, seven animals; artificial CSF + carbenoxolone, 0.298 ± 0.09, $n = 11$ cells, seven animals, $P = 0.006$) whereas carbenoxolone had no effect on ΔV_K in ipsilateral slices (artificial CSF, 0.193 ± 0.068, $n = 10$ cells, six animals; artificial CSF + carbenoxolone, 0.197 ± 0.055, $n = 12$ cells, seven animals, $P = 0.887$). The ipsi- and contralateral carbenoxolone values also differed significantly ($P = 0.003$). FV = fibre volley; *significantly different from the contralateral side (*t*-test); #significantly different from sham (ANOVA and Tukey test).

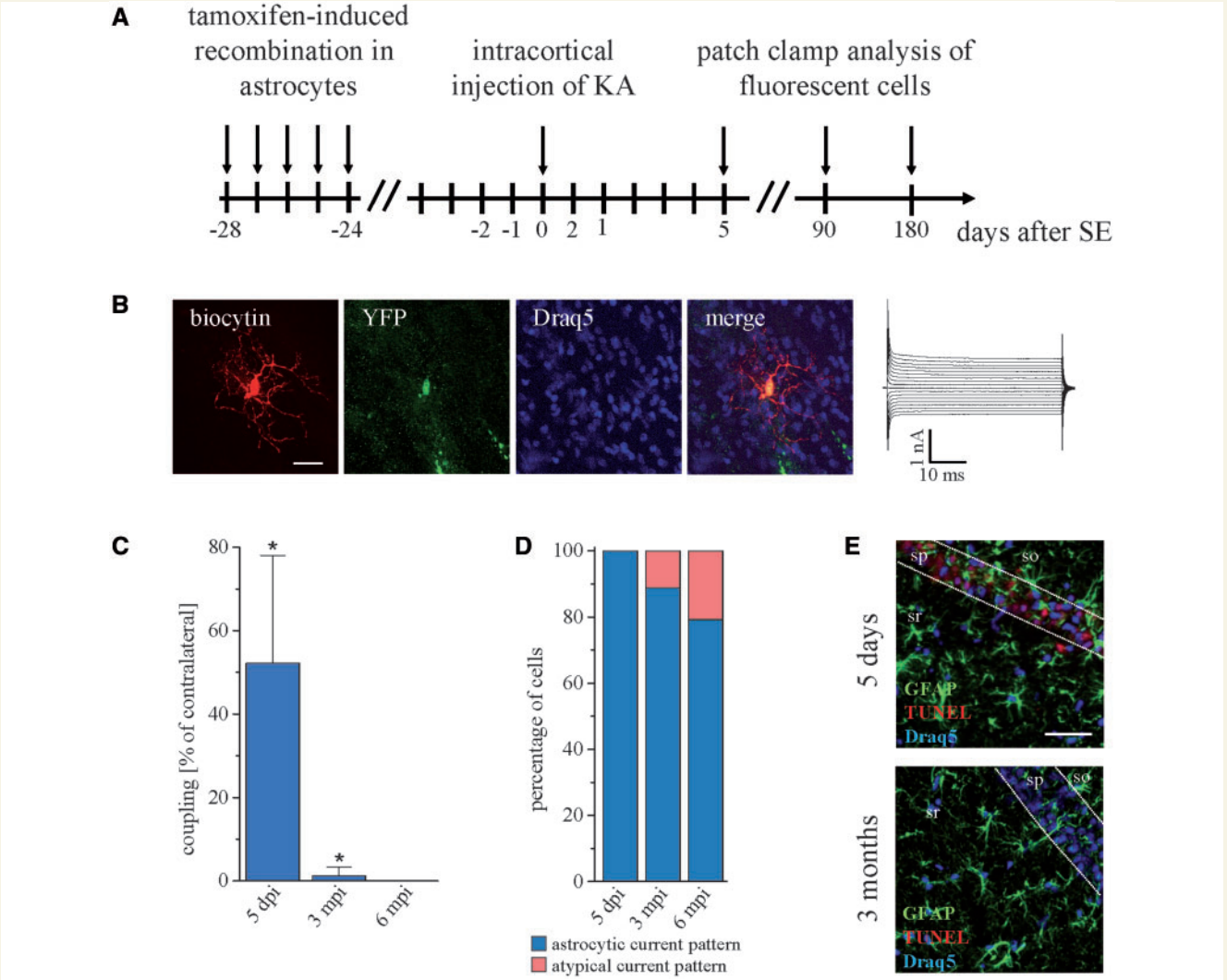

Figure 4 In the course of epilepsy astrocytes acquire an abnormal phenotype. (**A**) Schematic of fate mapping experiments. Activation of EYFP expression in GJA1-positive glial cells was induced by intraperitoneal injection of tamoxifen. Four weeks later, kainate was unilaterally injected into the cortex. Fluorescent cells were analysed electrophysiologically and immunohistochemically 5, 90 and 180 days after kainate injection. (**B**) Representative example of an EYFP-positive cell lacking gap junction coupling and showing abnormal input resistance (43 MΩ), distinct from *bona fide* astrocytes. Scale bar = 20 μm. (**C**) Tracer coupling analysis of EYFP-positive cells at different time points after kainate injection shows significant reduction of gap junction coupling already during the latent period (68.6 ± 33.9 versus 131.4 ± 33 coupled cells, $P = 0.009$, $n = 27$ slices from six animals), and complete loss of gap junction coupling after 6 months ($n = 22$ slices from five animals). (**D**) The proportion of EYFP-positive cells with membrane currents atypical for astrocytes increased with time after kainate injection (5 days post injection: $n = 30$ slices from six animals; 3 mpi: $n = 18$ slices from four animals; 6 mpi: $n = 24$ slices from six animals). (**E**) TUNEL/GFAP/Draq5 triple staining of coronal brain slices at 5 days and 3 months after kainate injection. No apoptotic astrocytes could be detected in sclerotic and non-sclerotic parts of ipsilateral hippocampi. sr = stratum radiatum; sp = stratum pyramidale; so = stratum oriens. Scale bar = 25 μm.

We used freshly resected hippocampal specimens from patients with MTLE to assess glial dysfunction in chronic human epilepsy. The astounding result of our comparative analysis is the complete absence in hippocampal sclerosis tissue of *bona fide* astrocytes, i.e. cells displaying a high resting conductance, passive current patterns and gap junction coupling. Remarkably, lack of astrocytes and gap junction coupling was seen in the hippocampus of all 75 patients with MTLE-HS, irrespective of their age, gender or medication, whereas robust coupling was present in all human non-hippocampal sclerosis specimens investigated. Some glial cells residing in MTLE-HS displayed atypical, 'intermediate' glutamate responsiveness, i.e. co-expression of ionotropic glutamate receptors and transporters. Immunohistochemistry did not indicate trans-differentiation of astrocytes into NG2 cells in MTLE-HS.

So far, gap junction coupling has not been assessed in human brain. In acute epilepsy models, release of glutamate from astrocytes promotes neuronal synchronization, and an excitatory neuron–astrocyte–neuron signalling cascade contributes to the initiation of focal ictal discharges (Gomez-Gonzalo *et al.*, 2010). However, acute models do

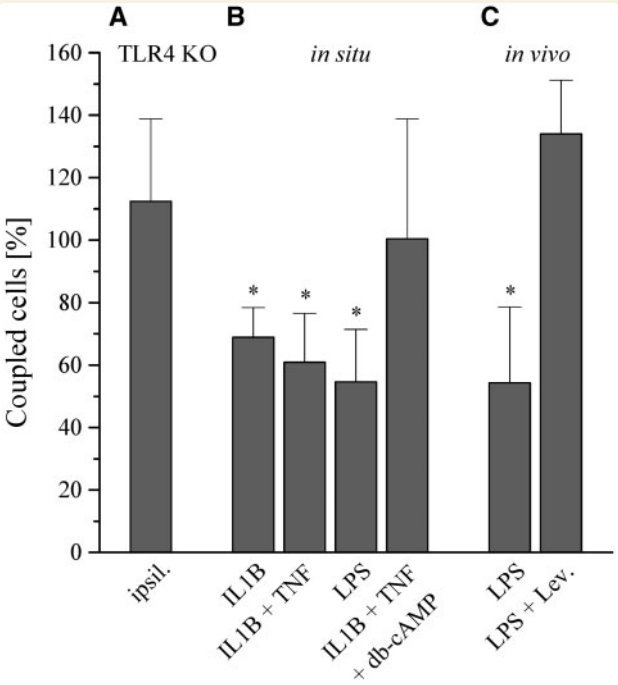

Figure 5 Pro-inflammatory cytokines and lipopolysaccharide inhibit astrocytic gap junction coupling. (**A**) Kainate injection did not affect astrocytic gap junction coupling in TLR4 knockout mice at 1 day post injection (121.2 ± 35.6 versus 115.9 ± 50.2 coupled cells, $P = 0.87$, $n = 10$ slices from five animals). Data were normalized to the contralateral side. Ipsi- and contralateral gap junction coupling were always compared in the same brain slices. (**B**) Tracer coupling analysis was performed *in situ* in acute brain slices 3–4.5 h after incubation with IL1B, IL1B/TNF (10 ng/ml), or lipopolysaccharide (LPS, 1 μg/ml). The cytokines and lipopolysaccharide significantly decreased gap junction coupling (control: 87.8 ± 18.2 coupled cells, $n = 33$ slices from 15 animals; IL1B: 60.5 ± 9.5 coupled cells, $P = 0.002$, $n = 10$ slices from seven animals; IL1B + TNF: 53.5 ± 15.6 coupled cells, $P < 0.0001$, $n = 15$ slices from 11 animals; lipopolysaccharide: 47.9 ± 16.8 coupled cells, $P = 0.0016$, $n = 14$ slices from four animals). The effect of the cytokines on gap junction coupling was prevented by addition of 100 μM dibutyryl cyclic AMP (IL1B + TNF + dibutyryl cyclic AMP: 88.2 ± 42.1 coupled cells, $P = 0.93$, $n = 18$ slices from six animals). Data were normalized to gap junction coupling in control slices (vehicle incubation). (**C**) *In vivo* effect of lipopolysaccharide on astrocytic gap junction coupling. Gap junction coupling was assessed in acute slices 5 days after i.p. injection of lipopolysaccharide (5 mg/kg). Lipopolysaccharide significantly decreased gap junction coupling (56.5 ± 27.5 coupled cells, $n = 21$ slices from five animals versus 104 ± 19 coupled cells, $n = 18$ slices from five animals, $P = 0.01$). Treatment of lipopolysaccharide-injected animals for 5 days with levetiracetam (150 mg/kg, i.p. two injections daily) fully restored gap junction coupling (139.3 ± 19.9 coupled cells, $P = 0.369$, $n = 19$ slices from five animals). Data were normalized to control mice (vehicle injection). *Significantly different (ANOVA and Tukey test); db-cAMP = dibutyryl cyclic AMP.

not mimic the morphological changes characterizing human MTLE-HS, including selective neuronal death, astrogliosis and granule cell dispersion. To determine the time course of the changes in astrocyte function in the course of human MTLE-HS and test whether they are causative for this disorder, a unilateral intracortical kainate model was used in mice. The ensuing long-term restructuring of the hippocampus observed up to 9 months post status epilepticus closely matched the morphological, molecular and functional features of the chronic stage of human MTLE-HS, including loss of passive astrocytes and coupling. Fate mapping analysis directly established that in the course of epilepsy, astrocytes acquire an atypical phenotype. We observed that astrocyte uncoupling is a very early event in epileptogensis and leads to impaired K^+ clearance. Importantly, these changes in astrocytes preceded apoptotic neuronal death and development of spontaneous recurrent seizures. Thus, dysfunction of astrocytes seems to play a key role in aetiology, and in this respect MTLE-HS may be considered a glial rather than a neuronal disorder.

Besides loss of coupling, which was complete 3 mpi, we observed a continuous increase in the proportion of cells with atypical current patterns beyond the 6-month time point. Although there was no further increase in seizure frequency between 6 and 9 months after status epilepticus, comparing the 3- and 9-month time points revealed a progression of CA1 pyramidal cell loss, granule cell dispersion and shrinkage of the CA1 pyramidal layer.

Indeed, the chronic sclerotic hippocampus is considered the most likely origin of chronic seizures in patients with temporal lobe epilepsy (De Lanerolle and Lee, 2005) although the underlying mechanisms are not fully understood (De Lanerolle *et al.*, 2012). In the latter review, excitable (spiking) NG2 cells were speculated to contribute to seizure generation, but our previous and current findings do not support this hypothesis. In our earlier study, current injections in glial cells of human sclerosis or in NG2 cells of human control samples never produced action potentials, and the Na^+ current densities were low (Hinterkeuser *et al.*, 2000). These previous findings are in line with the

present study where depolarization never elicited action potentials in glial cells. However, the lack of astrocyte coupling probably contributes to the enhanced extracellular glutamate and K^+ levels in human sclerosis as revealed by *in vivo* dialysis, which may entail a reduced threshold for the generation of hyperexcitablity and/or facilitate the spread of waves of depolarization from granule cells to the subiculum (De Lanerolle and Lee, 2005). In contrast, at early phases of epileptogenesis, when excitatory CA1 neurons are still in place, the decreased astrocyte coupling and impaired K^+ buffering identified in the present study may directly lead to neuronal hyperexcitability and seizure generation and thus play a causative role in the development of epilepsy.

In a previous report, Karadottir *et al.* (2008) reported that in rat cerebellar white matter, two types of NG2 cells co-exist, displaying or lacking action potentials and synaptic input. This has not been observed in control mouse (Matthias *et al.*, 2003) or human hippocampus (this study, see also Hinterkeuser *et al.*, 2000). Our fate mapping data (Fig. 4 and Supplementary Fig. 8) strongly suggest that the 'atypical' glial cells in human sclerosis, lacking coupling and co-expressing AMPA receptors and glutamate uptake, are transformed astrocytes and do not represent a distinct type of NG2 cells.

Increasing evidence suggests a contribution of inflammation to the pathophysiology of seizures (Vezzani *et al.*, 2011). Responses to acute seizures triggered by kainate induce rapid release of IL1B and TNF from microglia and astrocytes, and enhanced cytokine levels in serum and CSF have been found in epilepsy patients (Vezzani *et al.*, 2008). We observe that application of IL1B, TNF and lipopolysaccharide *in situ* and *in vivo* exert robust uncoupling effects on the glial network, which is in line with findings in cell culture (John *et al.*, 1999; Meme *et al.*, 2006). The high-mobility group box–TLR4 axis is involved in ictogenesis (Maroso *et al.*, 2010). Using TLR4 knockout mice we show here the critical involvement of this receptor in seizure-induced uncoupling of astrocytes. Importantly, preserved gap junction coupling in kainate-injected TLR4 knockout mice was not due to weaker status epilepticus as compared with wild-type mice.

Previous work has demonstrated that kainate application entails disruption of the blood–brain barrier and albumin extravasation, and the latter leads to activation of astroglial transforming growth factor beta 1 signalling and decreased astrocytic gap junction coupling (Braganza *et al.*, 2012). Whether these processes contribute to the uncoupling seen after kainate-induced status epilepticus in our model still needs to be investigated.

Astrocyte uncoupling might not only impair K^+ homeostasis but also enhance extracellular glutamate levels (Glass and Dragunow, 1995; Cavus *et al.*, 2005; Pannasch *et al.*, 2011). In addition to influencing coupling, IL1B and TNF are important factors in the regulation of glutamate uptake and release from astrocytes (Hu *et al.*, 2000; Bezzi *et al.*, 2001; Santello *et al.*, 2011). Thus, these cytokines may affect excitability through multiple glia-dependent pathways. Levetiracetam is a clinically approved antiepileptic drug that not only modulates neuronal properties but also exerts anti-inflammatory effects on glia, including reconstitution of gap junction coupling in cultured astrocytes (Haghikia *et al.*, 2008; Stienen *et al.*, 2011). The latter studies and our results suggest an antiepileptogenic effect of levetiracetam through its effect on astrocytic coupling. A previous study, employing systemic kainate injection to induce status epilepticus, observed that levetiracetam suppresses the development of spontaneous seizures (Sugaya *et al.*, 2010) whereas in an amygdala kindling rat model this antiepileptic drug did not prevent epileptogenesis (Brandt *et al.*, 2007). Differences in the experimental models (chemoconvulsant versus electrical stimulation-induced status epilepticus) likely account for this discrepancy. In a pilocarpine rat model, levetiracetam had variable effects in the chronic state (Glien *et al.*, 2002). Together, our findings add to the emerging view that astrocytes have a central role in the pathogenesis of epilepsy and, given the limited progress of neuron-centred epilepsy research over the past years, suggest astrocytic connexins as promising new targets for the development of alternative and more specific antiepileptic drugs. Identifying molecules that specifically act as connexin activators and rescue uncoupling would also allow proving a causal link between impaired gap junction communication and epileptogenesis.

Acknowledgements

We thank I. Mody, UCLA for comments on the manuscript, A. Vezzani, Milan for providing TLR4 ko mice, R. Jabs, Inst. Cell. Neurosci. Bonn, for help with SR101 staining, and A. Becker, Neuropathology Department, University of Bonn, for neuropathological assessment of human hippocampal specimens.

Funding

This work was supported by Deutsche Forschungsgemeinschaft, http://www.dfg.de (SFB/TR3, TP C1, C9; STE 552/3 to C.S.; SFB/TR3, TP C9 to M.T., SFB1089 B03 to C.H., SPP1757 HE6949/1 to C.H., EXC1086 to C.A.H.), European Union, http://cordis.europa.eu/fp7, http://www.esf.org (FP7-202167 NeuroGLIA, EuroEPINOMICS to C.S., ERA-Net NEURON CIPRESS to C.A.H.), NRW-Rückkehrerprogramm, http://www.wissenschaft.nrw.de/forschung/foerderung/wissenschaftlichen-nachwuchs-foerdern/rueckkehrerprogramm (to C.H.) and Human Frontiers Science Program, http://www.hfsp.org/ (to C.H.). The funders had no role in study design, data collection and analysis, decision to publish, or preparation of the manuscript.

The authors have no conflicting financial interests.

Supplementary material

Supplementary material is available at *Brain* online.

References

Akopian G, Kuprijanova E, Kressin K, Steinhäuser C. Analysis of ion channel expression by astrocytes in red nucleus brain stem slices of the rat. Glia 1997; 19: 234–46.

Behrens E, Zentner J, Van Roost D, Hufnagel A, Elger CE, Schramm J. Subdural and depth electrodes in the presurgical evaluation of epilepsy. Acta Neurochir (Wien) 1994; 128: 84–7.

Bergles DE, Jabs R, Steinhäuser C. Neuron-glia synapses in the brain. Brain Res Rev 2010; 63: 130–7.

Bergles DE, Jahr CE. Synaptic activation of glutamate transporters in hippocampal astrocytes. Neuron 1997; 19: 1297–308.

Braganza O, Bedner P, Hüttmann K, von Staden E, Friedman A, Seifert G, et al. Albumin is taken up by hippocampal NG2 cells and astrocytes and decreases gap junction coupling. Epilepsia 2012; 53: 1898–906.

Brandt C, Glien M, Gastens AM, Fedrowitz M, Bethmann K, Volk HA, et al. Prophylactic treatment with levetiracetam after status epilepticus: Lack of effect on epileptogenesis, neuronal damage, and behavioral alterations in rats. Neuropharmacology 2007; 53: 207–21.

Bezzi P, Domercq M, Brambilla L, Galli R, Schols D, De Clercq E, et al. CXCR4-activated astrocyte glutamate release via TNFalpha: amplification by microglia triggers neurotoxicity. Nat Neurosci 2001; 4: 702–10.

Bordey A, Sontheimer H. Properties of human glial cells associated with epileptic seizure foci. Epilepsy Res 1998; 32: 286–303.

Bouilleret V, Ridoux V, Depaulis A, Marescaux C, Nehlig A, La Salle GL. Recurrent seizures and hippocampal sclerosis following intrahippocampal kainate injection in adult mice: Electroencephalography, histopathology and synaptic reorganization similar to mesial temporal lobe epilepsy. Neuroscience 1999; 89: 717–29.

Cavus I, Kasoff WS, Cassaday MP, Jacob R, Gueorguieva R, Sherwin RS, et al. Extracellular metabolites in the cortex and hippocampus of epileptic patients. Ann Neurol 2005; 57: 226–35.

De Lanerolle NC, Lee TS. New facets of the neuropathology and molecular profile of human temporal lobe epilepsy. Epilepsy Behav 2005; 7: 190–203.

De Lanerolle NC, Lee TS, Spencer DD. Histopathology of human epilepsy. In: Noebels JL, Avoli M, Rogawski MA, Olsen RW, Delgado-Escueta AV, editors. Jasper's basic mechanisms of the epilepsies. 4th edn. Bethesda: Oxford University Press; 2012. p. 387–404.

Diamond JS. Deriving the glutamate clearance time course from transporter currents in CA1 hippocampal astrocytes: transmitter uptake gets faster during development. J Neurosci 2005; 25: 2906–16.

Djukic B, Casper KB, Philpot BD, Chin LS, McCarthy KD. Conditional knock-out of Kir4.1 leads to glial membrane depolarization, inhibition of potassium and glutamate uptake, and enhanced short-term synaptic potentiation. J Neurosci 2007; 27: 11354–65.

Eckardt D, Theis M, Degen J, Ott T, van Rijen HV, Kirchhoff S, et al. Functional role of connexin43 gap junction channels in adult mouse heart assessed by inducible gene deletion. J Mol Cell Cardiol 2004; 36: 101–10.

Eid T, Thomas MJ, Spencer DD, Runden-Pran E, Lai JC, Malthankar GV, et al. Loss of glutamine synthetase in the human epileptogenic hippocampus: possible mechanism for raised extracellular glutamate in mesial temporal lobe epilepsy. Lancet 2004; 363: 28–37.

Elger CE, Hufnagel A, Schramm J. Presurgical evaluation protocol—University of Bonn. In: Engel J Jr, editor. Surgical treatment of the epilepsies. New York: Raven Press; 1993. p. 740–2.

Giaume C, Koulakoff A, Roux L, Holcman D, Rouach N. Astroglial networks: a step further in neuroglial and gliovascular interactions. Nat Rev Neurosci 2010; 11: 87–99.

Glass M, Dragunow M. Neurochemical and morphological changes associated with human epilepsy. Brain Res Rev 1995; 21: 29–41.

Glien M, Brandt C, Potschka H, Löscher W. Effects of the novel antiepileptic drug levetiracetam on spontaneous recurrent seizures in the rat pilocarpine model of temporal lobe epilepsy. Epilepsia 2002; 43: 350–7.

Gomez-Gonzalo M, Losi G, Chiavegato A, Zonta M, Cammarota M, Brondi M, et al. An excitatory loop with astrocytes contributes to drive neurons to seizure threshold. PLoS Biol 2010; 8: e1000352.

Gosejacob D, Dublin P, Bedner P, Hüttmann K, Zhang J, Tress O, et al. Role of astroglial connexin30 in hippocampal gap junction coupling. Glia 2011; 59: 511–19.

Haghikia A, Ladage K, Hinkerohe D, Vollmar P, Heupel K, Dermietzel R, et al. Implications of antiinflammatory properties of the anticonvulsant drug levetiracetam in astrocytes. J Neurosci Res 2008; 86: 1781–88.

Halassa MM, Haydon PG. Integrated brain circuits: astrocytic networks modulate neuronal activity and behavior. Annu Rev Physiol 2010; 72: 335–55.

Henneberger C, Rusakov DA. Monitoring local synaptic activity with astrocytic patch pipettes. Nat Protoc 2012; 7: 2171–9.

Hinterkeuser S, Schröder W, Hager G, Seifert G, Blümcke I, Elger CE, et al. Astrocytes in the hippocampus of patients with temporal lobe epilepsy display changes in potassium conductances. Eur J Neurosci 2000; 12: 2087–96.

Hu S, Sheng WS, Ehrlich LC, Peterson PK, Chao CC. Cytokine effects on glutamate uptake by human astrocytes. Neuroimmunomodulation 2000; 7: 153–9.

John GR, Scemes E, Suadicani SO, Liu JSH, Charles PC, Lee SC, et al. IL-1β differentially regulates calcium wave propagation between primary human fetal astrocytes via pathways involving P2 receptors and gap junction channels. Proc Natl Acad Sci USA 1999; 96: 11613–18.

Kafitz KW, Meier SD, Stephan J, Rose CR. Developmental profile and properties of sulforhodamine 101-Labeled glial cells in acute brain slices of rat hippocampus. J Neurosci Methods 2008; 169: 84–92.

Karadottir R, Hamilton NB, Bakiri Y, Attwell D. Spiking and nonspiking classes of oligodendrocyte precursor glia in CNS white matter. Nat Neurosci 2008; 11: 450–6.

Kivi A, Lehmann TN, Kovacs R, Eilers A, Jauch R, Meencke HJ, et al. Effects of barium on stimulus-induced rises of $[K^+]o$ in human epileptic non-sclerotic and sclerotic hippocampal area CA1. Eur J Neurosci 2000; 12: 2039–48.

Lee SC, Liu W, Dickson DW, Brosnan CF, Berman JW. Cytokine production by human fetal microglia and astrocytes. Differential induction by lipopolysaccharide and IL-1 beta. J Immunol 1993; 150: 2659–67.

Liotta A, Rösner J, Huchzermeyer C, Wojtowicz A, Kann O, Schmitz D, et al. Energy demand of synaptic transmission at the hippocampal Schaffer-collateral synapse. J Cereb Blood Flow Metab 2012; 32: 2076–83.

Löscher W, Schmidt D. Modern antiepileptic drug development has failed to deliver: ways out of the current dilemma. Epilepsia 2011; 52: 657–78.

Maroso M, Balosso S, Ravizza T, Liu J, Aronica E, Iyer AM, et al. Toll-like receptor 4 and high-mobility group box-1 are involved in ictogenesis and can be targeted to reduce seizures. Nat Med 2010; 16: 413–19.

Matthias K, Kirchhoff F, Seifert G, Hüttmann K, Matyash M, Kettenmann H, et al. Segregated expression of AMPA-type glutamate receptors and glutamate transporters defines distinct astrocyte populations in the mouse hippocampus. J Neurosci 2003; 23: 1750–8.

Meeks JP, Mennerick S. Astrocyte membrane responses and potassium accumulation during neuronal activity. Hippocampus 2007; 17: 1100–108.

Meme W, Calvo CF, Froger N, Ezan P, Amigou E, Koulakoff A, et al. Proinflammatory cytokines released from microglia inhibit gap junctions in astrocytes: potentiation by beta-amyloid. FASEB J 2006; 20: 494–6.

Nagy JI, Rash JE. Connexins and gap junctions of astrocytes and oligodendrocytes in the CNS. Brain Res Rev 2000; 32: 29–44.

Nemani VM, Binder DK. Emerging role of gap junctions in epilepsy. Histol Histopathol 2005; 20: 253–9.

Nimmerjahn A, Kirchhoff F, Kerr JN, Helmchen F. Sulforhodamine 101 as a specific marker of astroglia in the neocortex *in vivo*. Nat Methods 2004; 1: 31–7.

Nolte C, Matyash M, Pivneva T, Schipke CG, Ohlemeyer C, Hanisch UK, et al. GFAP promoter-controlled EGFP-expressing transgenic mice: a tool to visualize astrocytes and astrogliosis in living brain tissue. Glia 2001; 33: 72–86.

Pannasch U, Vargova L, Reingruber J, Ezan P, Holcman D, Giaume C, et al. Astroglial networks scale synaptic activity and plasticity. Proc Natl Acad Sci USA 2011; 108: 8467–72.

Perea G, Navarrete M, Araque A. Tripartite synapses: astrocytes process and control synaptic information. Trends Neurosci 2009; 32: 421–31.

Riban V, Bouilleret V, Pham-Le BT, Fritschy JM, Marescaux C, Depaulis A. Evolution of hippocampal epileptic activity during the development of hippocampal sclerosis in a mouse model of temporal lobe epilepsy. Neuroscience 2002; 112: 101–11.

Santello M, Bezzi P, Volterra A. TNFalpha controls glutamatergic gliotransmission in the hippocampal dentate gyrus. Neuron 2011; 69: 988–1001.

Seifert G, Carmignoto G, Steinhäuser C. Astrocyte dysfunction in epilepsy. Brain Res Rev 2010; 63: 212–1.

Seifert G, Hüttmann K, Schramm J, Steinhäuser C. Enhanced relative expression of glutamate receptor 1 flip AMPA receptor subunits in hippocampal astrocytes of epilepsy patients with Ammon's horn sclerosis. J Neurosci 2004; 24: 1996–2003.

Seifert G, Schilling K, Steinhäuser C. Astrocyte dysfunction in neurological disorders: a molecular perspective. Nat Rev Neurosci 2006; 7: 194–206.

Simonato M, Löscher W, Cole AJ, Dudek FE, Engel J Jr., Kaminski RM, et al. Finding a better drug for epilepsy: Preclinical screening strategies and experimental trial design. Epilepsia 2012; 53: 1860–7.

Srinivas S, Watanabe T, Lin CS, William CM, Tanabe Y, Jessell TM, et al. Cre reporter strains produced by targeted insertion of EYFP and ECFP into the ROSA26 locus. BMC Dev Biol 2001; 1: 4.

Steinhäuser C, Jabs R, Kettenmann H. Properties of GABA and glutamate responses in identified glial cells of the mouse hippocampal slice. Hippocampus 1994; 4: 19–36.

Steinhäuser C, Seifert G, Bedner P. Astrocyte dysfunction in temporal lobe epilepsy: K+ channels and gap junction coupling. Glia 2012; 60: 1192–202.

Stienen MN, Haghikia A, Dambach H, Thone J, Wiemann M, Gold R, et al. Anti-inflammatory effects of the anticonvulsant drug levetiracetam on electrophysiological properties of astroglia are mediated via TGFbeta1 regulation. Br J Pharmacol 2011; 162: 491–507.

Sugaya Y, Maru E, Kudo K, Shibasaki T, Kato N. Levetiracetam suppresses development of spontaneous EEG seizures and abberant neurogenesis following kainate-induced status epilepticus. Brain Res 2010; 1352: 187–99.

Suzuki F, Junier M-P, Guilhem D, Sorensen J-C, Onteniente B. Morphogenetic effect of kainate on adult hippocampal neurons associated with a prolonged expression of brain-derived neurotrophic factor. Neuroscience 1995; 64: 665–74.

Theofilas P, Bedner P, Hüttmann K, Theis M, Steinhäuser C, Frank S. The proapoptotic BCL-2 homology domain 3-only protein Bim is not critical for acute excitotoxic cell death. J Neuropathol Exp Neurol 2009; 68: 102–10.

Vezzani A, Balosso S, Ravizza T. The role of cytokines in the pathophysiology of epilepsy. Brain Behav Immun 2008; 22: 797–803.

Vezzani A, French J, Bartfai T, Baram TZ. The role of inflammation in epilepsy. Nat Rev Neurol 2011; 7: 31–40.

Wallraff A, Odermatt B, Willecke K, Steinhäuser C. Distinct types of astroglial cells in the hippocampus differ in gap junction coupling. Glia 2004; 48: 36–43.

Wallraff A, Köhling R, Heinemann U, Theis M, Willecke K, Steinhäuser C. The impact of astrocytic gap junctional coupling on potassium buffering in the hippocampus. J Neurosci 2006; 26: 5438–447.

Zhang J, Dublin P, Griemsmann S, Klein A, Brehm R, Bedner P, et al. Germ-line recombination activity of the widely used hGFAP-Cre and nestin-Cre transgenes. PLoS One 2013; 8: e82818.